

See discussions, stats, and author profiles for this publication at: <https://www.researchgate.net/publication/261180248>

Synthesis of Sub-100-nm Liposomes via Hydration in a Packed Bed of Colloidal Particles

ARTICLE *in* INDUSTRIAL & ENGINEERING CHEMISTRY RESEARCH · DECEMBER 2013

Impact Factor: 2.59 · DOI: 10.1021/ie402567p

READS

44

2 AUTHORS, INCLUDING:



S.K. Sundar

Indian Institute of Technology Bombay

1 PUBLICATION 0 CITATIONS

SEE PROFILE

Synthesis of Sub-100-nm Liposomes via Hydration in a Packed Bed of Colloidal Particles

S. K. Sundar and Mahesh S. Tirumkudulu*

Department of Chemical Engineering, Indian Institute of Technology Bombay, Mumbai-400076, India

ABSTRACT: Drug delivery using liposomal carriers for targeting the afflicted areas of the host has attracted significant interest in the scientific community. While traditional liposome preparation techniques result in polydisperse suspension, postprocessing steps such as extrusion or filtering is required to obtain monodisperse liposomes in the sub-100-nm size range. Here, we describe a novel technique to synthesize monodisperse liposomes in the sub-100-nm size range using a packed bed of colloidal particles which could also be used to simultaneously encapsulate a drug. The methodology involves drying lipids dispersed in an organic solvent in a capillary packed with colloidal particles, which upon hydration with an aqueous buffer containing a drug leads to liposome formation with simultaneous encapsulation of the drug. Our experiments show that the size of the liposome is independent of the particle size or the pore size. The robustness of the process and the extremely tight control on the liposome size range make it amenable to point-of-care therapeutics involving liposomal drug delivery systems. We conclude with a discussion on the possible mechanisms for narrow size distribution of liposomes.

■ INTRODUCTION

It is well-known that when amphiphilic molecules are dispersed in water beyond a critical micellar concentration, they spontaneously aggregate into numerous structures such as micelles, bilayers, and vesicles depending on the relative strengths of hydrophobic and hydrophilic forces. Lipid molecules with two hydrophobic tails dispersed in an aqueous medium arrange into bilayers wherein the hydrophilic head groups of the two layers are exposed to the medium while the tails are directed inward in the gap between the head groups. The lipid membranes are common cellular structures and are actively involved in a number of biological functions. When the size of the bilayer exceeds a critical size, the energetically unfavorable edges exposed to the solvent are eliminated by the bilayer closing on itself to form a vesicle at the cost of relatively lower bending energy.¹ The vesicle/liposome structure has been exploited for numerous applications such as models for artificial cells, penetration enhancers in cosmetics, adjuvants for vaccination and in the food industry, and most commonly for encapsulating drugs for targeted delivery to the afflicted site, thereby minimizing drug loss and averting damage to healthy cells.²

One of the key aspects of using liposomes for drug delivery is its size, as it has been shown that the size of the drug carrying liposomes should be less than 100 nm to prevent their uptake by macrophages of the liver and the spleen.³ The synthesis of liposomes for drug delivery is typically achieved either mechanically by sonication or extrusion through small pores of large vesicles formed by hydration or chemically by varying the ionic strength or pH of the aqueous solution or by changing the solubility conditions.^{4–6} While each method has its advantages, most commercial applications of one or more of the aforementioned methods are carried out in environments where the characteristic length scales during the liposome formation are in millimeters or centimeters. Such processes result in heterogeneous size distribution which is subsequently eliminated via a final step of filtration to achieve the targeted

size range of 100 nm or lower. A comprehensive review of the various techniques for liposome synthesis and their relative advantages and disadvantages is presented by Lasic.⁷ More recently, microfluidics technology has been used to synthesize submicrometer liposomes via precise mixing of solvent stream containing the lipid and an aqueous stream.⁸ Confinement and a well-defined mixing environment enables continuous production of liposomes of sizes in the micrometer and submicrometer ranges. Thus, many of the above macroscale processes such as electroformation,⁹ hydration,¹⁰ extrusion,¹¹ and double emulsion technique¹² have been adapted to microfluidic devices, which allows better reproducibility and efficient use of reagents. New methodologies specific to the microfluidic environment such as the flow focusing technique of Jahn et al.,¹³ and a variant of the same but using membranes,¹⁴ have been able to synthesize monodisperse vesicles in the sub-100-nm range by varying the flow parameters. van Swaay and deMello⁸ in their review on the various microfluidic methods for forming liposomes stress the importance of simplicity or ease of use along with robustness as one of the main criteria for a process to be widely adopted. Microfluidic devices are often complex and difficult to operate, especially when many fluid inputs, different fluid phases, or complicated flow controls are required. Consequently, hydration followed by extrusion and/or filtration remains one of the preferred techniques industry-wide for synthesizing monodisperse liposomes in the sub-100-nm regime.

In this paper, we focus on the formation of liposomes via the hydration process to produce a sub-100-nm regime but with the eventual goal of eliminating the high shear homogenizing/extrusion and/or the filtering step from the synthesis process.

Received: August 6, 2013

Revised: November 4, 2013

Accepted: December 12, 2013

Published: December 12, 2013

The hydration process involves contacting dried lipid films with an aqueous solution which then undergo a complex process of unbinding of bilayer stacks from the lipid film. The process is a result of competition between steric repulsion and van der Waals attraction and is a function of temperature. At low temperatures, van der Waals forces dominate and the bilayers are tightly bound. However, with an increase in temperature, steric repulsion increases and beyond a critical temperature may exceed the attractive interaction leading to the unbinding of the bilayers.^{15,16} Several studies have attempted to produce monodisperse suspension of liposomes using the hydration route. Olson et al.¹⁷ have prepared multilamellar liposomes from a dry deposit of a mixture of lipids composed of phosphatidylserine, phosphatidylcholine, and cholesterol in a round bottomed flask. The multilamellar liposomes were subsequently extruded sequentially through filters of pore sizes ranging from 1 to 0.6 μm . Thus, the size was reduced from 1320 to 260 nm with a decrease in lamellarity. Hope et al.¹⁸ demonstrated the rapid production of monodisperse unilamellar vesicles of a size ranging from 56 to 243 nm where multilamellar liposomes obtained via hydration of dry lipid films were extruded through polycarbonate filters (30–400 nm pore size) under moderate pressures (≤ 500 lb/in²). Nayar et al.¹⁹ showed that the extrusion technique can also be extended to long-chain saturated phosphatidylcholines to obtain liposomes in the 60 nm range by multiple passes through 100-nm-pore filters. In all the above studies, it was found that the liposome size was dependent on the filter pore size and extrusion pressure and the process could be applied to both saturated and unsaturated lipid systems provided the extrusion is performed above the transition temperature of the lipid. More recently, Howse et al.²⁰ produced giant polymer liposomes of micrometer size from a templated surface made from poly(ethylene oxide)-co-poly(butylene oxide). The bilayer surface coated over the templated surface closes to form the liposome upon hydration, and the observed the liposome size could be obtained by equating the surface area of the polymer island to that of a sphere. Thus by varying the size of the polymer island, the liposome size can be controlled. While the aforementioned technique yields highly monodisperse vesicles directly via hydration without the need of extrusion, the scale-up of the process could be a challenge.

Here, we present a novel, one-step method based on the hydration technique to synthesize sub-100-nm liposomes with a low polydispersity index ($\text{PDI} \leq 0.2$) without the need for post processing. Lipid molecules initially dissolved in a solvent are dried in a packed bed of highly asymmetric colloidal particles with a rough surface and then hydrated to obtain a narrow size distribution of liposomes. It is shown that the final size distribution is independent of the flow rate of the hydrating medium, suggesting that extrusion is not the cause for the narrow size distribution of liposomes. Interestingly, when a milky white dispersion of large (micrometer range) and polydisperse liposomes is dried in the packed bed, rehydration with an aqueous buffer yields a monodisperse liposome dispersion in the sub-100-nm size range. The final size distribution is independent of the size of the colloidal particles and the packing fraction in the bed, suggesting that the liposome size may be determined by the highly asymmetric particle shape and the structure of the porous packing. We believe that the robustness of the one-step hydration process, the absence of postprocessing, and the extremely tight control

on the liposome size range makes it amenable to point-of-care therapeutics involving liposomal drug delivery systems.

MATERIALS AND METHODS

Materials. 1,2-Dimyristoyl-sn-glycero-3-phosphocholine (DMPC) and 1,2-dipalmitoyl-sn-glycero-3-phosphocholine (DPPC) were obtained in solution form from Avanti Polar Lipids, Alabama. Sodium chloride, potassium chloride, disodium hydrogen orthophosphate, and potassium dihydrogen orthophosphate were obtained from Sigma Aldrich and used without any further purification. Solvents (chloroform and methanol) used to dissolve lipid were of a high grade and obtained from Merck Chemicals. The α -alumina particles (AKP-15, AKP-30, and AKP-50) were obtained from Sumitomo Chemicals, Japan. Circular glass capillaries of 0.5 mm i.d. and 4 mm o.d. and of length 100 mm were obtained from Arte Glass (Japan). Circular glass capillaries of 2 mm i.d. and 4 mm o.d. and of length 100 mm were used for the packed bed experiments and were obtained from a local supplier.

Preparation of Packed Bed. The alumina particles of each grade were monodisperse ($\text{PDI} < 0.1$) but not spherical. The average sizes of the particles of AKP-15, AKP-30 and AKP-50, as determined by dynamic light scattering (DLS), were 600 nm, 350 nm, and 250 nm, respectively (see Figure 1). We quantified

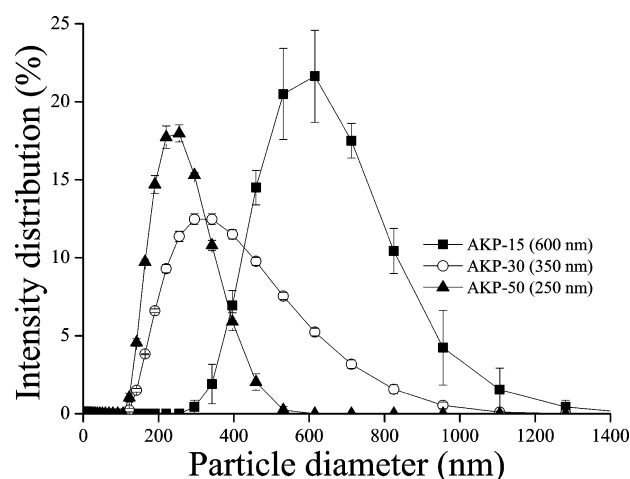


Figure 1. Size (diameter) distribution (by intensity) for the three different grades of α -alumina particles.

the shape, and therefore the asymmetry, of the alumina particles from scanning electron microscopy images in terms of circularity, which is defined as 4π times the ratio of the area of the particle to the square of its perimeter. A circularity value of 1.0 indicates a perfect circle and therefore a spherical object. The circularity of all three particle sizes was found to be about 0.74.

Dilute aqueous dispersion (35% of particles by volume) of high-purity α -alumina was prepared by dispersing it in deionized water. The pH of the dispersion was adjusted using analytical-grade HNO_3 and KOH to obtain dispersions with pH 2, 5, and 9. The 2-mm-i.d. capillary was placed vertically and filled with the dispersion from the top using a syringe or a micropipet, while the bottom end was closed with 200 nm filter paper. The latter prevent the particles from flowing out of the bottom of the capillary. The capillary was left to dry in the vertical position, during which the particles consolidate and concentrate via sedimentation and drying. Knowing the initial

dilute dispersion length in the capillary (l_0) and particle volume fraction ($\phi_0 = 0.35$), the final dried packing volume fraction (ϕ_f) was obtained from volume balance, $l_f \phi_f = l_0 \phi_0$, where l_f is the measured final length of the dried particle packing in the capillary. The particle volume fraction in the dried packing was varied by choosing initial dispersions with varying pH. As has been shown by Singh et al.,²¹ the zeta potential of alumina particles is high and positive at low pH and decreases with increasing pH, reaching the isoelectric point at pH 9. Consequently, at a pH of 2, the dispersion is stable and yields a dried particle packing fraction of 0.7 while the particles flocculate at pH 9, resulting in a dried particle packing fraction of about 0.3. Once the particle packing had completely dried, the filter paper was removed and the capillary, with both ends open, was placed in an oven at 1100 °C for 30 to 60 min so that the particles sinter slightly, thereby giving mechanical integrity to the packing. There was no visible change in the inner diameter of the capillary post-sintering. After complete sintering, the capillary was cut into 3-cm sections, which was eventually used for hydration experiments. Note that in all cases, the entire 3 cm section of the capillary was packed with sintered particles. We also determined the particle volume fraction in the bed post-sintering by saturating the sintered particle bed with water and noting the change in weight of the capillary. Since the total volume of the inside of the capillary was known, the volume of water imbibed inside the sintered bed was used to determine the particle volume fraction of the bed post-sintering. The sintering process increased the particle volume fraction by about 10% to 20%—from 0.56 to 0.61 for pH 2, from 0.42 to 0.52 for pH 5, and from 0.35 to 0.45 for pH 9, irrespective of the particle type. About 5 mL of ultrapure and sterile Milli-Q water was passed through the freshly sintered packed bed using a syringe pump (NE-1000, New Era Pump Systems), and the fluid was collected for dynamic light scattering (DLS) measurements. The DLS reading of the Milli-Q water before and after passage through the bed was identical with very low count rate, suggesting the absence of particles, and thereby confirming that the alumina particles were firmly embedded in the packing.

Liposome Preparation and Size Distribution. Two different sets of experiments were performed to synthesize liposomes via hydration. In the first case, hollow circular cross-sectional capillaries of 0.5 mm inner diameter and 100 mm length were coated with a thin film of lipid on the inner surface followed by hydration with an aqueous buffer. In the second set, capillaries with a packed bed of colloids were used instead of the hollow capillaries for liposome preparation. Most of the experiments were carried out with DMPC (gel–liquid crystal transition temperature, $T_c = 23$ °C) at a temperature, T_{exp} , of 29 °C. The experimental protocol for the packed bed is shown in Figure 2. About 50 μ L of lipid solution is dispensed into the packed bed using a micropipette. Next, the capillary is dried with nitrogen gas for about 10 min. Here, a standard laboratory nitrogen cylinder operating at a pressure of about 0.3 bar is connected to a 4 mm i.d. Teflon tube. The other end of the Teflon tube is connected to a 0.2 μ m filter (Millipore) which in turn is connected to the capillary containing the sintered bed of particles. The filter prevents possible dust particles in the nitrogen line from entering the bed. The dried lipid bilayers are subsequently hydrated with a phosphate buffer with the latter dispensed separately using a syringe pump. A 5 mL syringe was used in all experiments. A 4 mm i.d. connector made of Teflon was affixed to the syringe outlet, which in turn was connected

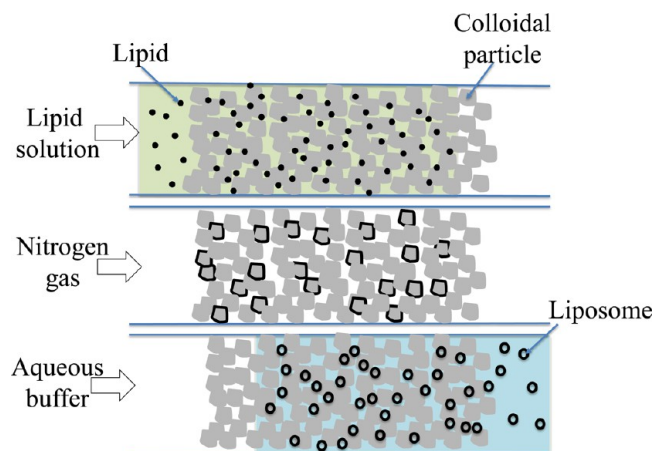


Figure 2. Schematic representation of experimental setup. Lipid dissolved in a solvent is introduced into the packed bed. The solvent is dried in a stream of nitrogen gas, leaving behind a coating of lipid bilayers on the particles. Finally, an aqueous buffer hydrates the bilayer to form liposomes.

to the capillary. The joints at the two ends of the connector were tightly sealed using Teflon tape to prevent leakage of the hydration medium. The phosphate buffer used for hydration contained for 1 L of buffer, 8.01 g of NaCl, 0.20 g of KCl, 1.44 g of Na_2HPO_4 , and 0.24 g of KH_2PO_4 . The phosphate buffer was sterilized by filtering it through a 0.22 μ m filter before performing the experiments. The experiments were performed inside laminar flow hood that create a dust-free environment. The experimental procedure for hydration through the 0.5 mm i.d. hollow capillary (i.e., without packed bed) was identical. We measured the back pressure immediately downstream of the syringe during hydration of the packed bed for the range of flow rates used in our experiments. The pressure values were in the range of 1 to 5 bar for the three packings.

The buffer solution containing liposomes was collected and analyzed using dynamic light scattering. The experiments were performed for buffer flow rates, Q , of 20 μ L/min, 60 μ L/min, 150 μ L/min, and 200 μ L/min; lipid concentrations, C_o , of 10 mM, 35 mM, and 70 mM; and packing volume fractions of 0.35, 0.42, and 0.56 for packed beds of AKP-30 (350 nm) particles. For the remaining two particle beds (AKP-15 and AKP-50), experiments were conducted at $Q = 20$ μ L/min, $C_o = 70$ mM, and $\phi_f = 0.35$.

Transmission Electron Microscopy (TEM), Scanning Electron Microscopy (SEM), and Atomic Force Microscopy (AFM). Apart from using dynamic light scattering to determine the liposome size distribution, the liposomes were also imaged in the cryogenic mode using both TEM and SEM. Sample preparation for Cryo-TEM involves placing a small drop of the liposome sample in the grid and removing the excess solution using filter paper, a process termed blotting. The grid is immediately plunged into liquid ethane for vitrification. The grid is transferred to grid holder and stored under liquid nitrogen until analysis. For Cryo-SEM, a small drop of the sample was placed on the sample holder and then plunged into liquid nitrogen. The freeze-dried sample was sublimed for around 5 min before imaging.

The sintered alumina packing was platinum coated for 30 s and observed under SEM to determine particle packing and the extent of sintering. The circularity of the particles was estimated from the SEM image using Image J software and is defined as

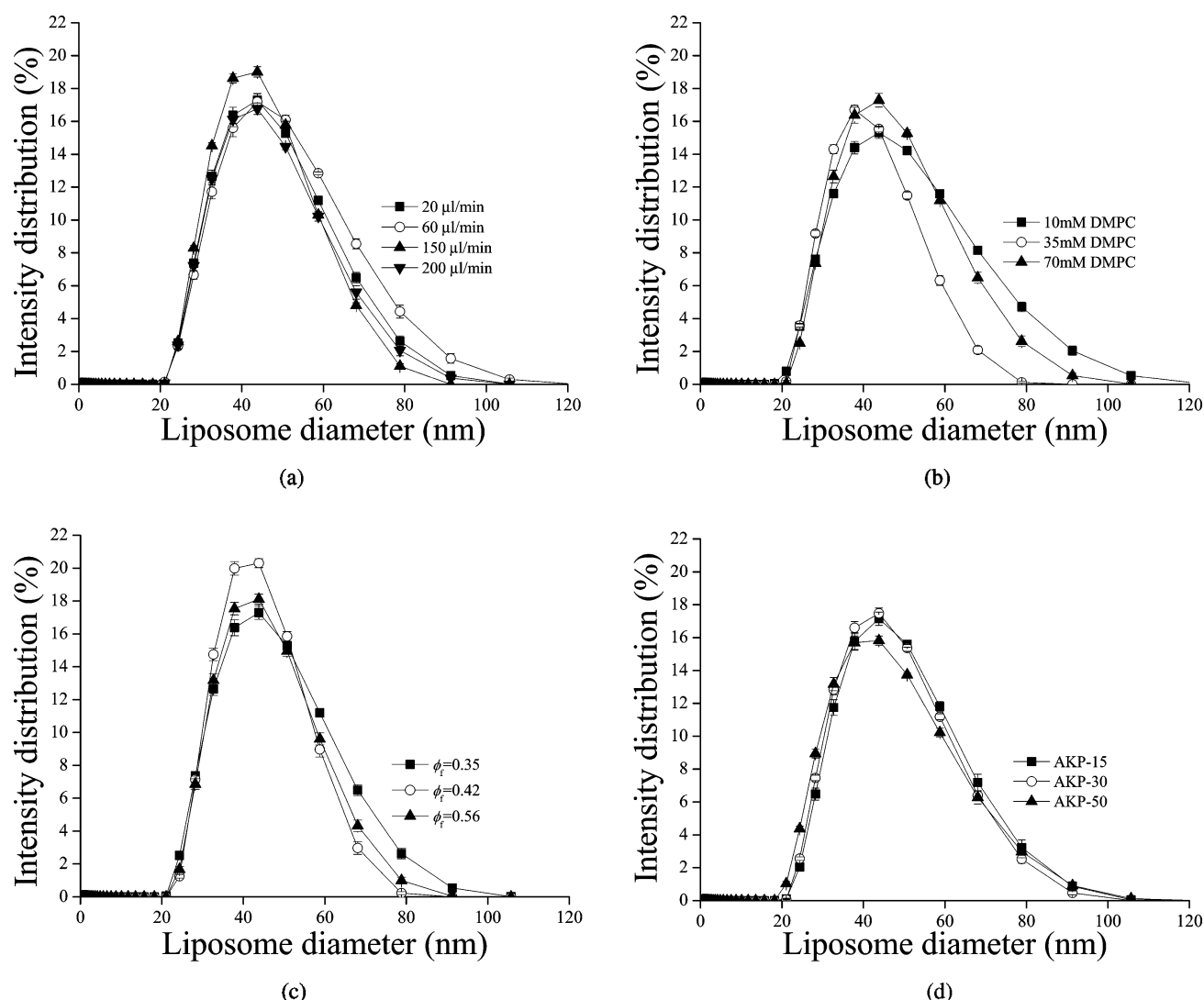


Figure 3. Plots showing size (diameter) distribution (by intensity) of liposomes of DMPC with variation in (a) flow rate of the buffer for $C_o = 70$ mM in a packed bed of AKP-30 particles at $\phi_f = 0.35$, (b) lipid concentration for $Q = 20 \mu\text{L}/\text{min}$ in a packed bed of AKP-30 particles at $\phi_f = 0.35$, (c) volume fraction of particles in a packed bed of AKP-30 particles for $Q = 20 \mu\text{L}/\text{min}$ and $C_o = 70$ mM, and (d) particle size for a packing fraction of $\phi_f = 0.35$, $Q = 20 \mu\text{L}/\text{min}$, and $C_o = 70$ mM.

4 π times the ratio of the area of the particle to the square of its perimeter. A circularity value of 1.0 indicates a perfect circle.

We characterized the surface topology of films prepared from alumina particles using atomic force microscopy (AFM). Dispersions containing the three different grades of alumina particles were coated and dried over separate silicon wafers followed by sintering at 1100 °C for 1 h. The topology of the film was obtained using the AFM.

RESULTS AND DISCUSSION

Hydration experiments performed with hollow capillaries resulted in a polydisperse suspension of liposomes with a high PDI of ~ 0.8 , irrespective of lipid concentration or buffer flow rate (results not shown). These results are not entirely surprising given that the experimental conditions are similar to those obtained via the standard technique of hydration in a round-bottom flask.¹⁷ On the other hand, experiments involving packed beds yielded highly monodisperse liposomes with a narrow size distribution in the sub-100-nm range. Figure 3 presents the liposome size distribution (intensity plot from

DLS) for varying buffer flow rate, lipid concentration, packed bed particle volume fraction, and size of particles in the packed bed. Each experiment was repeated three times to confirm the reproducibility of the results. In all cases, the distribution peaks at about 50 nm, with a PDI of less than 0.2 indicating that the final distribution is highly monodisperse irrespective of the variation in the parameters. Interestingly, the distributions are very similar, thereby suggesting that there is no significant influence of the parameters on the final liposome size distribution.

In order to confirm the size range measured using DLS, the sample was imaged using both Cryo-TEM and Cryo-SEM. Figure 4a shows the image of liposomes formed for DMPC of $C_o = 70$ mM and $Q = 20 \mu\text{L}/\text{min}$ in a bed packed with AKP-30 particles at $\phi_f = 0.35$. All liposomes visible in the image lie in the 10–40 nm size range. Further, a close inspection of the TEM images shows that all the liposomes are unilamellar. Figure 4b includes a cryo-SEM image of the sample obtained under identical experimental conditions. Note that the former exhibits a lower density of liposomes due to the blotting technique employed during sample preparation for cryo-TEM.

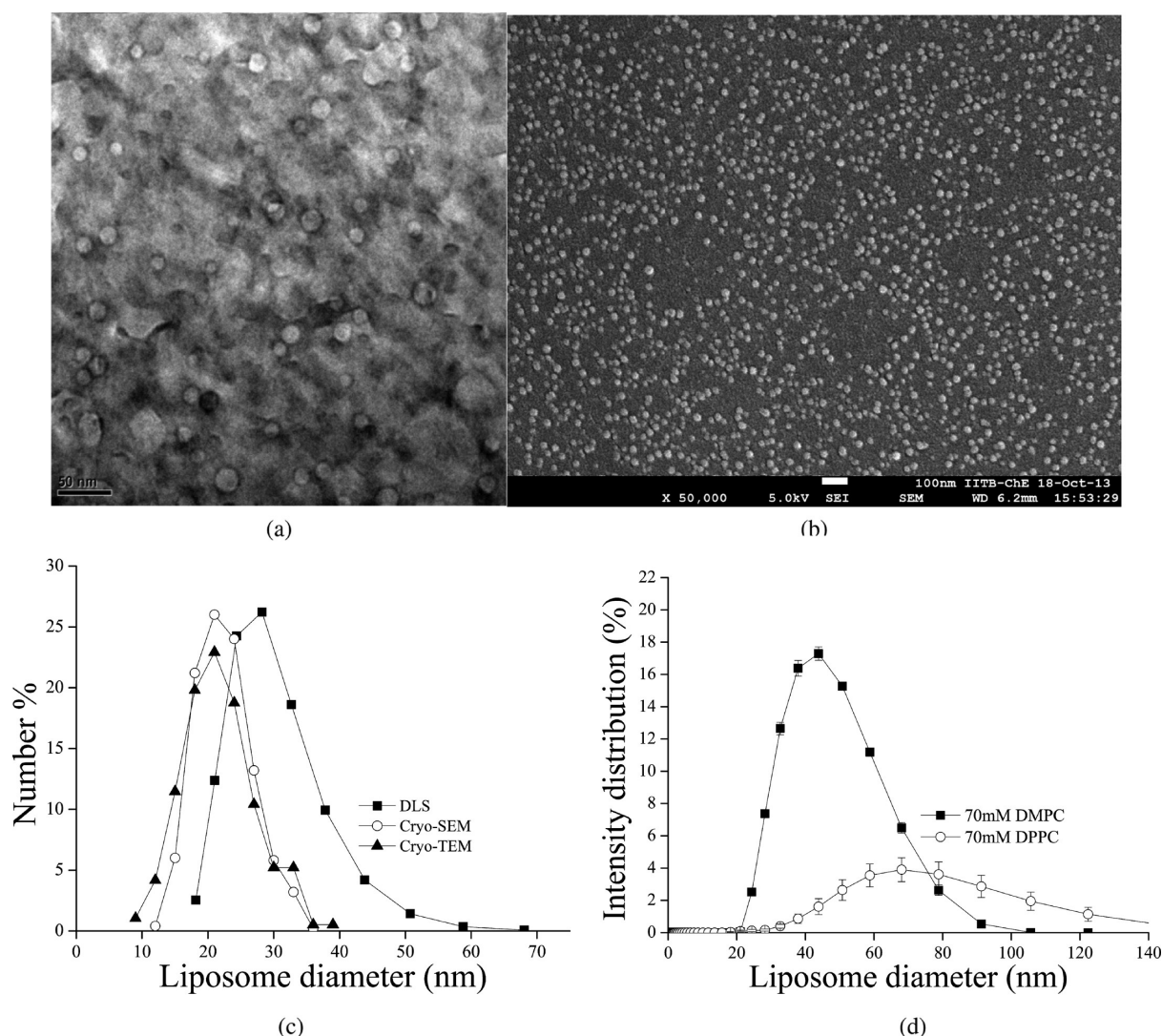


Figure 4. (a) Cryo-TEM image of liposomes obtained from a 70 mM DMPC lipid in a bed packed with AKP-30 particles, $\phi_f = 0.35$, $Q = 20 \mu\text{L}/\text{min}$. (b) Cryo-SEM image of liposomes obtained from 70 mM DMPC lipid in bed packed with AKP-30 particles, $\phi_f = 0.35$ at a flow rate of $20 \mu\text{L}/\text{min}$ and temperature 29°C . (c) Plot showing liposome size (diameter) distribution (by number) obtained from cryo-TEM, cryo-SEM, and DLS. (d) Size (diameter) distribution (by intensity) of liposomes of DMPC ($T_c = 23^\circ\text{C}$, $T_{\text{exp}} = 29^\circ\text{C}$) and DPPC ($T_c = 41^\circ\text{C}$, $T_{\text{exp}} = 48^\circ\text{C}$) from 70 mM lipid concentration in bed packed with AKP-30 particles, $\phi_f = 0.35$ at a flow rate of $20 \mu\text{L}/\text{min}$.

In Figure 4c, we compare the distribution obtained from DLS with that obtained from image analysis of both the Cryo-TEM and Cryo-SEM images. All three distributions indicate that the majority of the liposomes fall in the range of 20–50 nm.

To determine if the size distribution of the liposomes is specific to the lipid, experiments were also performed with DPPC, with $T_c = 41^\circ\text{C}$, in a packed bed of AKP-30 particles in an oven maintained at $T_{\text{exp}} = 48^\circ\text{C}$ (Figure 4d). The liposome size distribution was again in the same range as that observed for DMPC for the same lipid concentration and buffer flow rate, indicating that the size distribution may not be specific to a particular lipid. When experiments were performed at temperatures more than 20°C above T_c , liposome average size increased to about 200 nm and with high polydispersity.

The extrusion of large multilamellar liposomes through porous membranes has shown that the size of the extruded liposomes is only slightly larger than the pore size of the membranes.²² In order to determine if the extrusion is the cause for the sub-100-nm liposomes in our experiments, a SEM image of the packed particles in the bed was taken to determine

the pore size in the packing. Figure 5 clearly shows that the particles are uniformly packed and the pore size increases with particle size, suggesting that irrespective of the pore size the liposome size distribution remains unchanged. Further, liposomes synthesized from particle beds sintered for 30 and 60 min did not show any difference in size.

Extrusion Is Not the Cause for Small Unilamellar Liposomes. While the experiments demonstrate that hydration in beds of different particle sizes does not influence the final liposome size, it also appeared that the liposome size was not influenced by flow through the pores while being extruded through the bed. In order to test this hypothesis, two different sets of experiments were performed. First, a preformed liposome suspension of peak size around 600 nm with $\text{PDI} \leq 0.2$ was extruded through a packed bed of AKP-30 particles. Interestingly, there was no difference in the size distribution upon extrusion as shown in Figure 6a. Second, 100 μL of DMPC lipid in chloroform at a concentration of 70 mM was dried in a vial followed by gentle hydration with the phosphate buffer. The milky white dispersion containing highly poly-

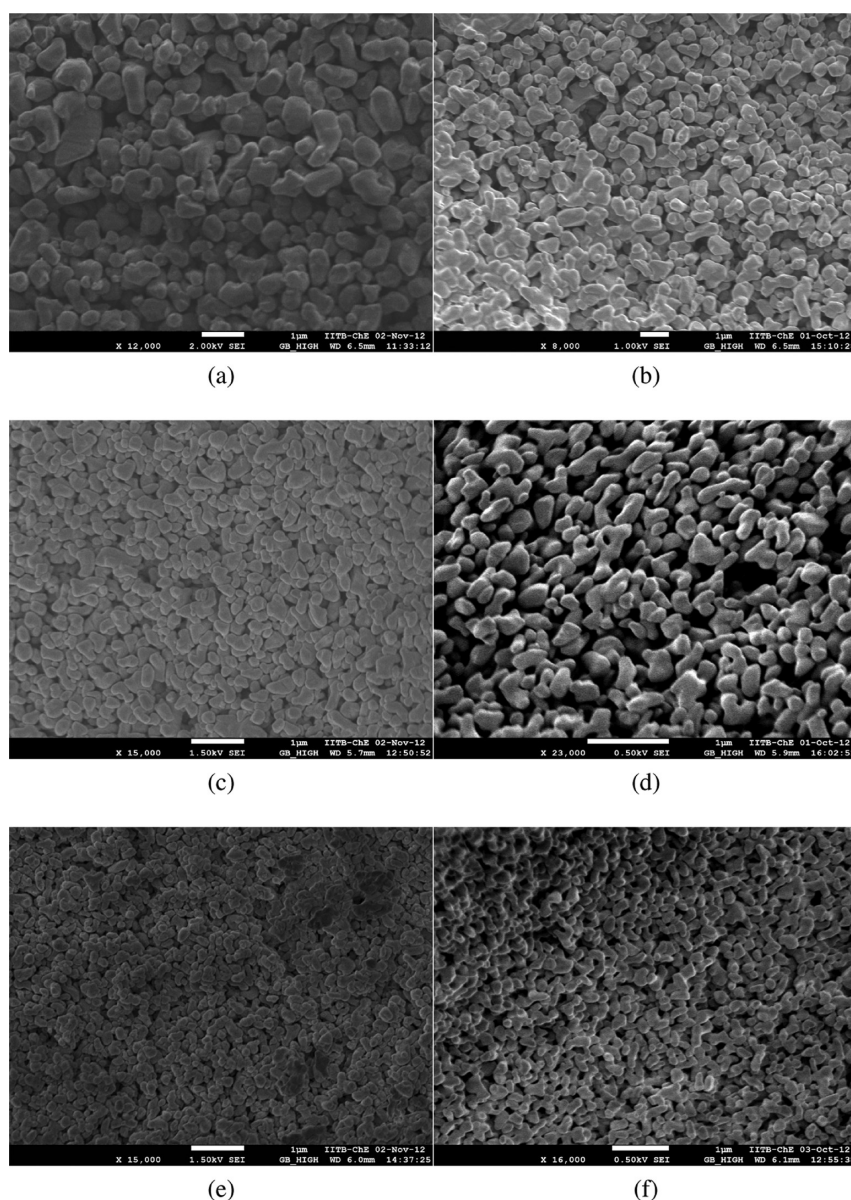


Figure 5. SEM images of (a) AKP-15 (30 min sintering). (b) AKP-15 (60 min sintering). (c) AKP-30 (30 min sintering). (d) AKP-30 (60 min sintering). (e) AKP-50 (30 min sintering). (f) AKP-50 (60 min sintering).

disperse liposomes was introduced into the packed bed and dried with nitrogen gas. When the bed was rehydrated with the buffer, a monodisperse liposome dispersion with a sub-100-nm size distribution was obtained (see Figure 6b). Both these experiments clearly demonstrate that extrusion is not responsible for the observed size range.

The experimental evidence seems to suggest that the liposome size is set during the hydration stage and subsequent passage through the bed has no effect on the size. Since the liposome size was also found to be independent of the particle size and therefore the pore size (see Figure 3), we speculate that the final size is determined by a combination of the length scale of the internal topology of the packing and the bending modulus of the bilayer. Thermodynamically, the smallest possible liposome size is set by a balance of the edge energy of flat circular bilayer and the bending energy required for the bilayer to fold into a sphere of radius R_v assuming that the two structures have the same surface area.²³

$$R_v = \frac{2K_b + K_G}{\lambda}$$

where K_b is the bending modulus, K_G is the modulus due to the Gaussian curvature, and λ is the edge energy due to the exposed hydrocarbon tails along the perimeter of the bilayer. Molecular dynamics simulation of bilayers formed with pure DMPC predicts²⁴ $\lambda \sim 10\text{--}30$ pN. K_b at 30 °C has been measured to be²⁵ 1.15×10^{-19} J, while the ratio of the Gaussian modulus to the bending modulus is taken as²⁶ $K_b/K_G \sim -1$. Substituting these values in the above equation gives the minimum liposome diameter for DMPC to be 23 nm, which is close to the smallest sizes observed in the measured distributions (Figure 3).

While the above calculation explains the smallest observed liposome size, the reasons for the occurrence of a peak size of 50 nm (measured via DLS) with a majority of the liposomes in the sub-100-nm size range are not clear. Recent experiments by Roiter et al.²⁷ have investigated the interaction of lipid membranes of DMPC with nanostructured surfaces formed

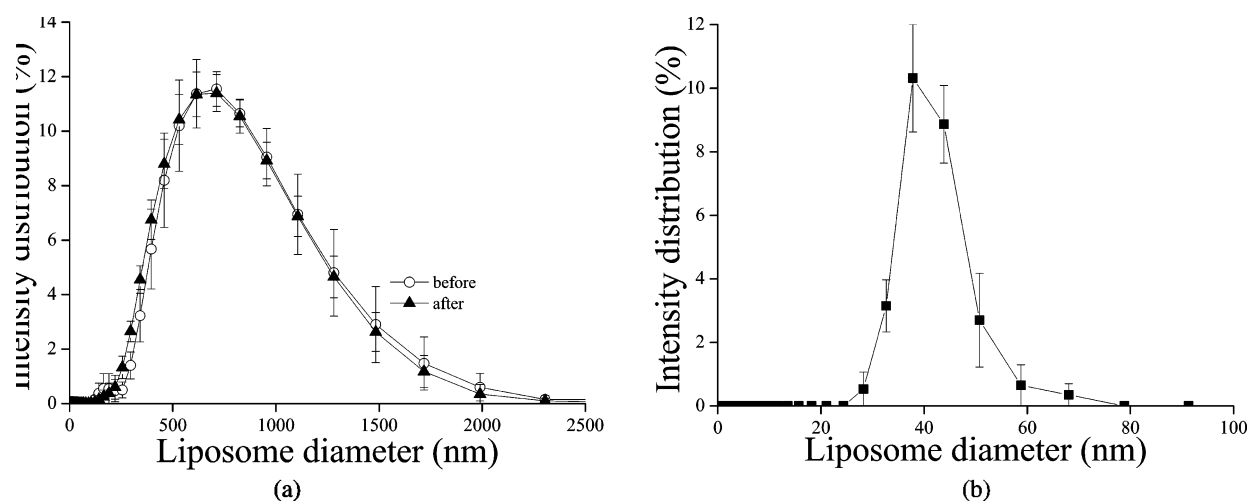


Figure 6. Size (diameter) distribution (by intensity) of liposomes of DMPC (a) before and after extrusion and (b) after rehydration through a bed packed with AKP-30 particles, $\phi_i = 0.35$ at a flow rate of $20 \mu\text{L}/\text{min}$ and a temperature of 29°C .

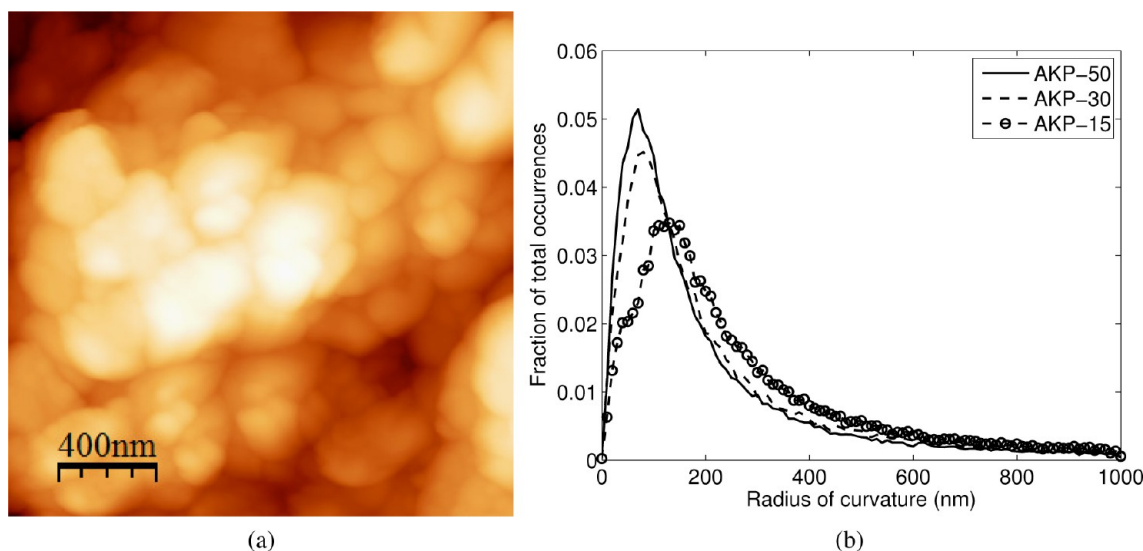


Figure 7. (a) Surface topology of a surface coated with AKP-30 particles obtained using AFM. (b) Fraction of total occurrences of mean curvature for surfaces with the three different alumina particles for a bin size of 10 nm.

by depositing silica nanoparticles of different diameters on plane and smooth silica substrates. They show that lipid membranes can completely coat smooth silica particles with diameters greater than 22 nm, but for nanostructured dimensions between 1.2 and 22 nm, the lipid membrane developed pores (holes) suggesting that continuous membranes are energetically unfavorable compared to the energy penalty for exposing the hydrophobic edge of the bilayer.

In order to determine whether the surface roughness could be the cause for the sub-100-nm liposomes, dispersions of alumina particles were coated and dried over silicon wafers followed by sintering at 1100°C for 1 h. AFM was performed over the sintered surface (Figure 7a) over a scan area of $2 \mu\text{m} \times 2 \mu\text{m}$, and the height data were used to determine the mean curvature at all the height points over the surface.²⁸ Figure 7b plots the fraction of total occurrences for radii of curvature (taken as the inverse of mean curvature) from 0 to 1000 nm with a bin size of 10 nm. The fractional occurrences rise sharply at low radii of curvature reaching a peak at 70, 80, and 130 nm for AKP-50, AKP-30, and AKP-15, respectively, and decrease

slowly for higher values. The profiles for the three particles are very similar, suggesting that the topology of the film is independent of the particle size. Further, almost 40% of the coating surface has a radius of curvature less than 100 nm for the smallest particle (AKP-50), while it is about 20% for AKP-15, suggesting that the rough surface of individual particles leads to significantly large regions with a radius of curvature smaller than the particle size. Irrespective of the particle type, not more than 30% of the surface had radii of curvature greater than 300 nm. Given that the radii of curvature is expected to be even lower inside the porous packing due to its three-dimensional nature, the rough surface of the highly asymmetric particles along with the porous nature of the packing may result in patchy coatings of membranes on the particles that subsequently unbind and close upon hydration to give sub-100-nm liposomes. Future experiments involving alumina particles of varying roughness/asymmetry would be required to establish the hypothesis. Finally, the hydration technique demonstrated here can easily be modified into a continuous process to produce drug-encapsulated liposomes. Alternate

liquid plugs of lipid solution and aqueous buffer (containing a drug) pumped through a packed bed will result in a continuous stream of liquid plug carrying sub-100-nm liposomes. We estimated the volume fraction of vesicles produced using this technique. Assuming that a monolayer of lipid coats the entire particle surface in the packing along with complete saturation of the bed with a buffer, the volume fraction of the vesicles is estimated to be about 0.10 for an average vesicle diameter of 50 nm and a spherical alumina particle of diameter 350 nm. However, the concentration of the liposomes and therefore the encapsulation efficiency can be increased by decreasing the ratio of the volume of the buffer to the lipid volume.

CONCLUSION

We demonstrate a novel liposome preparation technique suitable for continuous production of unilamellar liposomes with low polydispersity ($PDI \leq 0.2$) in a single step. It is shown that the final size distribution is independent of the size of the colloidal particles, packing fraction in the bed, or the flow rate of the hydrating medium, suggesting that extrusion is not the cause for the narrow size distribution of liposomes. Experiments suggest that the high asymmetry of the particles along with the porous structure of the packing may play a critical role in determining the final liposome size distribution. We believe that the extremely narrow size distribution in the sub-100-nm range makes the liposome synthesis technique described here be directly applicable to point-of-care therapeutics involving liposomal drug delivery systems, thereby eliminating problems related to postprocessing and the short shelf life of liposomal formulations.

AUTHOR INFORMATION

Corresponding Author

*E-mail: mahesh@che.iitb.ac.in.

Notes

The authors declare no competing financial interest.

ACKNOWLEDGMENTS

We acknowledge the IRHPA program of the Department of Science and Technology, India for financial support, SAIF and Chemical Engineering Department of IIT Bombay for TEM and SEM, and the Central SPM facility of IITB for use of AFM.

REFERENCES

- (1) Israelachvili, J. N. *Intermolecular and Surface Forces*; Academic Press: New York, 2011.
- (2) Mouritsen, O. *Life - As a Matter of Fat*; Springer-Verlag: New York, 2005.
- (3) Drummond, D. C.; Meyer, O.; Hong, K.; Kirpotin, D. B.; Papahadjopoulos, D. Optimizing Liposomes for Delivery of Chemotherapeutic Agents to Solid Tumors. *Pharmacol. Rev.* **2009**, 6287.
- (4) Bangham, A.; Standish, M.; Watkins, J. Diffusion of univalent ions across the lamellae of swollen phospholipids. *J. Mol. Biol.* **1965**, 13, 238.
- (5) Deamer, D.; Bangham, A. Large volume liposomes by an ether vaporization method. *Biochim. Biophys. Acta* **1976**, 443, 629.
- (6) Szoka, F.; Papahadjopoulos, D. Procedure for preparation of liposomes with large internal aqueous space and high capture by reverse-phase evaporation. *Proc. Natl. Acad. Sci. U. S. A.* **1978**, 75, 4194.
- (7) Lasic, D. D. *Liposomes: From Physics to Applications*; Elsevier: Amsterdam, 1993.
- (8) van Swaay, D.; deMello, A. Microfluidic methods for forming liposomes. *Lab Chip* **2013**, 13, 752.
- (9) Le Berre, M.; Yamada, A.; Reck, L.; Chen, Y.; Baigl, D. Electroformation of Giant Phospholipid Vesicles on a Silicon Substrate: Advantages of Controllable Surface Properties. *Langmuir* **2008**, 24, 2643.
- (10) Lin, Y.; Huang, K.; Chiang, J.; Yang, C.; Lai, T. Manipulating self-assembled phospholipid microtubes using microfluidic technology. *Sens. Actuators, B* **2006**, 117, 464.
- (11) Dittrich, P. S.; Heule, M.; Renaud, P.; Manz, A. On-chip extrusion of lipid vesicles and tubes through micro-sized apertures. *Lab Chip* **2006**, 6, 488.
- (12) Teh, S.; Khnouf, R.; Fan, H.; Lee, A. P. Stable, biocompatible lipid vesicle generation by solvent extraction-based droplet microfluidics. *Biomicrofluidics* **2011**, 5, 044113.
- (13) Jahn, A.; Vreeland, W.; Devoe, D.; Locascio, L.; Gaitan, M. Microfluidic directed formation of liposomes of controlled size. *Langmuir* **2007**, 23, 6289.
- (14) Akamatsu, K.; Shimizu, Y.; Shimizu, R.; Nakao, S.-i. Facile Method for Preparing Liposomes by Permeation of Lipid-Alcohol Solutions through Shirasu Porous Glass Membranes. *Ind. Eng. Chem. Res.* **2013**, 52, 10329.
- (15) Pozo-Navas, B.; Raghunathan, V.; Katsaras, J.; Rappolt, M.; Lohner, K.; Pabst, G. Discontinuous unbinding of lipid bilayers. *Phys. Rev. Lett.* **2003**, 91, 028101-1.
- (16) Yamada, N.; Hishida, M.; Seto, H.; Tsumoto, K.; Yoshimura, T. Unbinding of Lipid Bilayers Induced by Osmotic Pressure in Relation to Unilamellar Vesicle Formation. *Europhys. Lett.* **2007**, 80, 480002-p1.
- (17) Olson, F.; Hunt, C.; Szoka, F.; Vail, W.; Papahadjopoulos, D. Preparation of liposomes of defined size distribution by extrusion through polycarbonate membranes. *Biochim. Biophys. Acta* **1979**, 557, 9.
- (18) Hope, M.; Bally, M.; Webb, G.; Cullis, P. Production of large unilamellar vesicles by a rapid extrusion procedure. Characterization of size distribution, trapped volume and ability to maintain a membrane potential. *Biochim. Biophys. Acta* **1985**, 812, 55.
- (19) Nayar, R.; Hope, M. J.; Cullis, P. R. Generation of large unilamellar vesicles from long-chain saturated phosphatidylcholines by extrusion technique. *Biochim. Biophys. Acta* **1989**, 986, 200.
- (20) Howse, J. R.; Jones, R. A. L.; Battaglia, G.; Ducker, R. E.; Leggett, G. J.; Ryan, A. J. Templated formation of giant polymer vesicles with controlled size distributions. *Nat. Mater.* **2009**, 8, 507.
- (21) Singh, K. B.; Bhosale, L. R.; Tirumkudulu, M. S. Cracking in Drying Colloidal Films of Flocculated Dispersions. *Langmuir* **2009**, 25, 4284.
- (22) Mayer, L.; Hope, M.; Cullis, P. Vesicles of variable sizes produced by a rapid extrusion procedure. *Biochim. Biophys. Acta, Biomembr.* **1986**, 858, 161.
- (23) Boal, D. *Mechanics of the Cell*; Cambridge University Press: Cambridge, U. K., 2001.
- (24) Jiang, F. Y.; Bouret, Y.; Kindt, J. T. Molecular Dynamics Simulations of the Lipid Bilayer Edge. *Biophys. J.* **2004**, 87, 182.
- (25) Duwe, H. P.; Kaes, J.; Sackmann, E. Bending elastic moduli of lipid bilayers: modulation by solutes. *J. Phys. (Paris)* **1990**, 51, 945.
- (26) Hu, M.; de Jong, D. H.; Marrink, S. J.; Deserno, M. Gaussian curvature elasticity determined from global shape transformations and local stress distributions: a comparative study using the MARTINI model. *Faraday Discuss.* **2013**, 161, 365.
- (27) Roiter, Y.; Ornatska, M.; Rammohan, A. R.; Balakrishnan, J.; Heine, D. R.; Minko, S. Interaction of Lipid Membrane with Nanostructured Surfaces. *Langmuir* **2009**, 25, 6287.
- (28) Gray, A. *Modern Differential Geometry of Curves and Surfaces with Mathematica*; CRC Press: Boca Raton, FL, 1997.